Geophysical Research Letters

RESEARCH LETTER
10.1029/2018GL078212

Observations and Modeling of Long-Period Ground-Motion Amplification Across Northeast China

Haichao Chen[1,2], **Victor C. Tsai**[2], **and Fenglin Niu**[1,3]

[1]Unconventional Natural Gas Institute and State Key Laboratory of Petroleum Resources and Prospecting, China University of Petroleum, Beijing, China, [2]Seismological Laboratory, California Institute of Technology, Pasadena, CA, USA, [3]Department of Earth, Environmental and Planetary Sciences, Rice University, Houston, TX, USA

Key Points:
- Long-period ground motions are significantly amplified within sedimentary basins in northeast China
- Site amplification of surface waves is distinctly different from that of vertically incident shear waves
- The amplification of both shear waves and surface waves can be quantitatively explained by accounting for the effects of local one-dimensional structure

Supporting Information:
- Supporting Information S1
- Data Set S1

Correspondence to:
H. Chen,
chchao@cup.edu.cn

Citation:
Chen, H., Tsai, V. C., & Niu, F. (2018). Observations and modeling of long-period ground-motion amplification across northeast China. *Geophysical Research Letters, 45*, 5968–5976. https://doi.org/10.1029/2018GL078212

Received 5 APR 2018
Accepted 2 JUN 2018
Accepted article online 8 JUN 2018
Published online 22 JUN 2018

Abstract Basin resonances can significantly amplify and prolong ground shaking, and accurate site-amplification estimates are crucial for mitigating potential seismic hazards within metropolitan basins. In this work, we estimate the site amplification of long-period (2–10 s) ground motions across northeast China for both surface waves and vertically incident shear waves. The spatial distribution of relatively large site amplifications correlates strongly with known sedimentary basins for both wave types. However, the site response of surface waves is typically twice as high as that of shear waves at most basin sites. We further show that these site-amplification features can be well explained by predictions based on the local one-dimensional structure at each site. Our results highlight the importance of accounting for surface-wave contributions and demonstrate the usefulness of semi-analytical theory for surface-wave amplification, which may be broadly applicable in future seismic hazard analysis.

Plain Language Summary Surface waves are often the dominant wave type observed for large shallow earthquakes at relatively large distances. Surface-wave amplification at sites underlain by thick, soft sediments within the Songliao basin is substantially larger than in adjacent generic rock sites in northeast China. This highlights the importance of accounting for the contributions of surface waves in accurately predicting earthquake ground motions. A semi-analytic method for estimating surface-wave amplification can well explain the most significant site-amplification features, based on the local one-dimensional structure at each site. This approach may be broadly applicable in future seismic hazard analysis.

1. Introduction

Basin resonances are well-recognized seismic hazards, which can significantly amplify and prolong long-period ($<$ 1 Hz) ground motions from moderate to large regional events (e.g., Asano et al., 2016; Borcherdt, 1970; Galetzka et al., 2015) and thus potentially cause devastating damage to large manmade constructions, for example, high-rise buildings, large-storage oil tanks, and long-span bridges (Hatayama, 2008; Kano et al., 2017; Pratt et al., 2017). Usually, the seismic response of sedimentary basins from large shallow earthquakes is dominated by surface waves. Therefore, accurate estimate of surface-wave amplification is an important practical need for mitigating potential seismic hazards in metropolitan areas atop sediment-filled basins.

Unfortunately, it is not a trivial task to quantitatively model the amplification of surface waves. Since surface waves are excited and propagate differently as compared to vertically incident shear waves, they have a distinctly different frequency-dependent response to known geologic structure (Bowden & Tsai, 2017). Hence, the standard one-dimensional (1-D) ground response analysis, which considers the effect of near-surface geology on vertically propagating shear waves or simply uses empirical proxies (e.g., Vs30), often underestimates the observed amplifications (e.g., Steidl, 2000). Moreover, site amplification across deep sedimentary basins could be highly variable even over distances of a few kilometers (Imperatory & Mai, 2015; Moschetti et al., 2017), which is often attributed to three-dimensional (3-D) basin effects related to how basin shape and lateral heterogeneities affect wave propagation (Graves et al., 1998; Kawase, 1996; Pilz et al., 2018; Takemura et al., 2015). As such, much effort has been devoted to 3-D numerical simulations of earthquake ground motions in sedimentary basins (e.g., Böse et al., 2014; Chaljub et al., 2015; Frankel et al., 2009; Iwaki & Iwaka, 2010; Olsen, 2000; Olsen et al., 2006; Pilz et al., 2011). Such basin resonance effects can also be captured by observations of the ambient seismic field (e.g., Bowden et al., 2015; Denolle, Dunham, et al.,

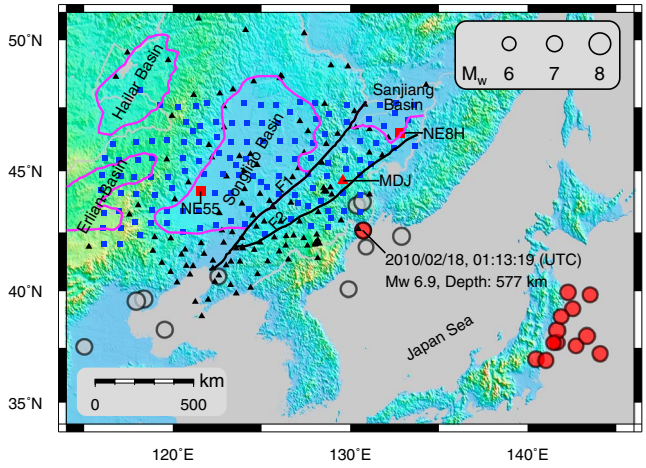

Figure 1. Map view of northeast China. The magenta lines delineate the outlines of the major basins in northeast China, and black lines indicate the active faults. The gray circles represent large historical earthquakes. The red circles denote the earthquake events used in this study, including the 12 shallow regional events off the coast of Japan and one deep local event (577 km) beneath northeast China. These signals were captured by the temporary broadband array (blue squares) and the permanent stations (black triangles) that covered the study area. The red triangle and the two red squares denote the reference station at a bedrock site (IC.MDJ) and two typical basin stations used in Figures 2, S1, S2, and S3, respectively.

2014; Denolle, Miyake, et al., 2014; Viens et al., 2016). Recently, Bowden and Tsai (2017) proposed a semi-analytical method to estimate surface-wave amplification relative to a reference bedrock site, using the local 1-D shallow structure at a specific site. Within the framework of this theory, Tsai et al. (2017) successfully explained the extreme ground motions in Osaka basin due to the great 2011 Tohoku earthquake. This novel approach provides a simple way to estimate the site amplification of surface waves in a manner similar to current engineering practice of seismic hazard assessment, without requiring computationally intensive 3-D waveform modeling.

Northeast China is one of the most densely populated regions in China and sits atop several alluvial basins, including the central Songliao basin and the eastern Sanjiang basin (Figure 1). The Songliao basin, about 750 km long and 330–370 km wide, hosts the largest nonmarine oil field in China (Daqing Oilfield). In particular, most of the petroleum reservoirs are located in the central down warp of the Songliao basin (Feng et al., 2010), which also appears to possess the thickest sediments inside the basin (Li et al., 2016). Unfortunately, this earthquake-prone region is bounded in the southeast by several active faults (black lines) and is frequently subject to strong shaking from a diversity of earthquake sources (Duan et al., 2017), as exemplified by a series of large earthquakes of magnitude up to 7.5 in the 1960s and 1970s (gray circles). Thus, accurate estimates of ground-motion amplification would make an important contribution to quantifying the seismic hazard from potential *M*7+ earthquakes in the study region. In this work, we characterize the site amplification of long-period ground motions across northeast China. Specifically, we aim to understand and quantitatively explain the distinctly different amplifications of surface waves within the sedimentary basins, as compared to vertically incident shear waves.

2. Data and Methodology

2.1. Site Amplification Estimation

We use earthquake records from a temporary broadband array deployed across northeast China (blue squares in Figure 1), complemented by permanent seismic stations (black triangles), to obtain frequency-dependent site-amplification measurements of both surface waves and vertically propagating shear waves (Figure 2a). The large-scale broadband array, known as the NECESSArray (NorthEast China Extended SeiSmic Array), consists of 126 temporary broadband stations with an average station spacing of approximately 80 km that covers most of northeast China (Tao et al., 2014). It was deployed between September 2009 and August 2011 under an international collaborative project and captured the great 2011 Tohoku earthquake off the coast of Japan and subsequent large aftershocks (red circles in Figure 1; Table S1 in the supporting information). These shallow undersea earthquakes generated strong long-period surface waves that swept across the region of interest. In fact, most of the broadband stations clipped during the great Tohoku earthquake even more than 1,000 km away from the epicenter, with peak velocities exceeding 1 cm/s. In order to circumvent the difficulty of separating surface waves from body waves, we use observed velocity records from a deep earthquake of magnitude 6.9 beneath the study area (Figure 1), which hardly excited surface waves, to estimate the site amplification of vertically incident shear waves.

It has been the standard practice in earthquake engineering to calculate the site amplification relative to a bedrock reference site (e.g., Borcherdt, 1970; Borcherdt & Gibbs, 1976). Here we calculate the response spectral ratio, instead of the standard spectral ratio, to obtain smoother site response over the frequency range of interest (Roten et al., 2013). The only permanent GSN station in the study area, IC.MDJ, was chosen as the reference site due to its extremely low level of background noise (Figure 1). Taking a typical basin site (YP.NE8H) as an example, the detailed procedures for estimating site amplification are presented in Text S1.

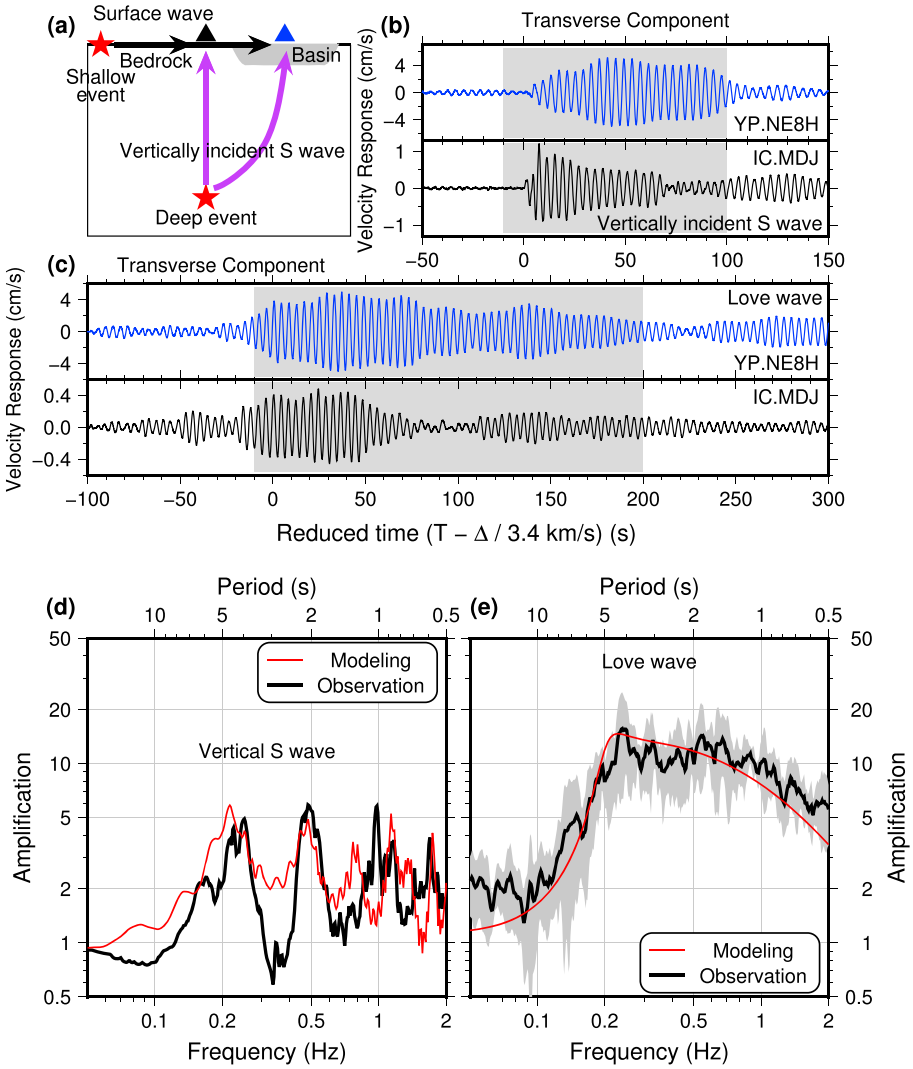

Figure 2. (a) Schematic showing the distinct propagation of surface waves and body waves. Shear waves from the deep local earthquake propagate nearly vertically as they reach the surface (purple arrows), whereas surface waves from the shallow regional events enter laterally and travel across the basin (black arrows). (b, c) Example velocity response at a period of 4 s for (b) the deep local event (shear wave) and (c) one shallow regional event at one typical basin site (YP.NE8H, top panels) and the reference site (IC.MDJ, bottom panels). The traces are plotted with absolute amplitudes in units of cm/s, with the gray shadow indicating the time window used for calculating the response spectra. It is noted that the reduced velocity of 3.4 km/s corresponds to the average group velocity of the Love waves at a period of 4 s. (d, e) Example comparison of the observed (thick black lines) and predicted (thin red lines) site amplification curves for (d) the vertically incident shear wave and (e) the fundamental-mode Love wave, at the same basin site as in panels (b) and (c). The gray shadow in panel (e) denotes ±1 standard deviation of the average response spectral ratio for Love waves. Note that the predictions of both wave types are in good agreement with the observed amplifications, in terms of both peak amplification factors and resonance frequencies.

2.2. Modeling Site Amplification

The site response term for vertically incident shear waves can be semi-analytically estimated using a Thomson-Haskell propagator matrix approach (Haskell, 1953; Kramer, 1996). In this study, we further employ the semi-analytical method of Bowden and Tsai (2017) to quantitatively explain the observed surface-wave amplifications across northeast China. Consistent with the current standard practice in earthquake engineering for site-specific analysis, this novel method also calculates the local site amplification of surface waves using the local 1-D shallow velocity and density structure at a specific site. Conservation of surface-wave energy flux requires that the relative amplitudes of surface waves with respect to a reference site satisfy (Aki & Richards, 2002; Tromp & Dahlen, 1992)

$$\frac{A}{A_R} = \frac{u(0)}{u_R(0)} \left(\frac{UI}{U_R I_R} \right)^{-1/2} \quad (1)$$

where $u(0)$ is the displacement eigenfunction at the surface, U is the group velocity, and I is an energy integral over the eigenfunction and density for the mode considered. The subscript R denotes the measurements at a reference site. This theory accounts for both Rayleigh and Love waves that propagate laterally through a smoothly varying medium (e.g., the basin of interest). Note that the I integrals are defined differently for Rayleigh and Love waves. The readers are referred to Bowden and Tsai (2017) and Tsai et al. (2017) for a detailed derivation of equation (1). Here we emphasize that the expression A/A_R defines a frequency-dependent transfer function by which surface-wave ground motions at a reference site can be transformed to another one, solely using the local 1-D structure. While it is unlikely that a single transfer function can capture the full variability of the entire surface-wave system in a realistic 3-D structure, this simple method provides first-order estimates of surface-wave amplification, in the absence of full 3-D numerical simulations. In our study, the local 1-D velocity structure beneath each temporary station was previously obtained using joint inversion of Rayleigh-wave ellipticity and surface-wave dispersion data from both ambient noise and earthquakes at periods of 8–40 s (Li et al., 2016). Like with the observations, for the modeling we also use the 1-D structure at the MDJ site outside the Songliao basin as the reference site to calculate the predicted site amplification. Figures S4 and S5 present the modeled amplification of fundamental-mode surface waves at two typical basin sites (YP.NE8H and YP.NE55), respectively. The site amplification of vertically incident shear waves is also shown for comparison. Apparently, the resonance frequencies of all wave types at station YP.NE8H are relatively lower than those at station YP.NE55, due to much thicker near-surface sediments (~2 km) beneath station YP.NE8H. In addition, the peak amplification of the Love wave is greater than that of the shear wave by a factor of 2 for both sites, despite the comparable fundamental resonance frequencies.

3. Results

3.1. Frequency-Dependent Site Amplification

Figure 2b displays the velocity response at a period of 4 s for the deep local earthquake (shear wave) from the basin site YP.NE8H (top) and the reference site (bottom), respectively. Similar results for one shallow regional earthquake (surface wave) is presented in Figure 2c. It is obvious that the durations of ground shaking of both events at the basin site are significantly longer because of multiple reflections. Moreover, the peak response of the surface wave at the basin site (top panel) is larger than that of the reference site (bottom panel) by an order of magnitude, whereas that of the shear wave at the basin site is only larger by a factor of ~5. Figures 2d and 2e show a comparison between the observed (black lines) and predicted (red lines) site amplification at the same basin site, for the vertically incident shear wave and the fundamental-mode Love wave, respectively. It is clear from the comparison that the predictions of both wave types are in good agreement with the observed amplifications, in terms of both peak amplification factors and resonance frequencies. Interestingly, the modeled Love-wave amplification even fits the shape of the observed amplification reasonably well. While there is significant amplification over the long period range between 1 and 10 s for both wave types, the site response for Love waves is distinctly different from that of the vertically incident shear wave. The shear-wave site amplification exhibits multiple resonance peaks, with peak amplification factors of approximately 5 at the primary and first overtone resonance frequencies around 4 and 2 s, which likely originate from reverberations within near-surface reflective layers. Conversely, the Love wave is amplified by a factor of 15 at the fundamental resonance frequency (~4 s), with a broader range of periods that also have substantial amplification.

3.2. Spatial Variability of Site Amplification

Figure 3 demonstrates the spatial variability of the observed amplification at periods of 2–3 s for vertically incident shear waves, Love waves, and horizontal-component and vertical-component Rayleigh waves, respectively. We calculate the amplification factors by averaging over the narrow period range of interest. The lateral variations of site amplification clearly delineate the known geological structures, for example, the central Songliao basin and the eastern Sanjiang basin (magenta lines). Generally, the site amplification at generic bedrock sites is less than 1.5. In contrast, the ground motions of both Love waves and horizontal-component Rayleigh waves within the Songliao basin can be amplified by a maximum factor of

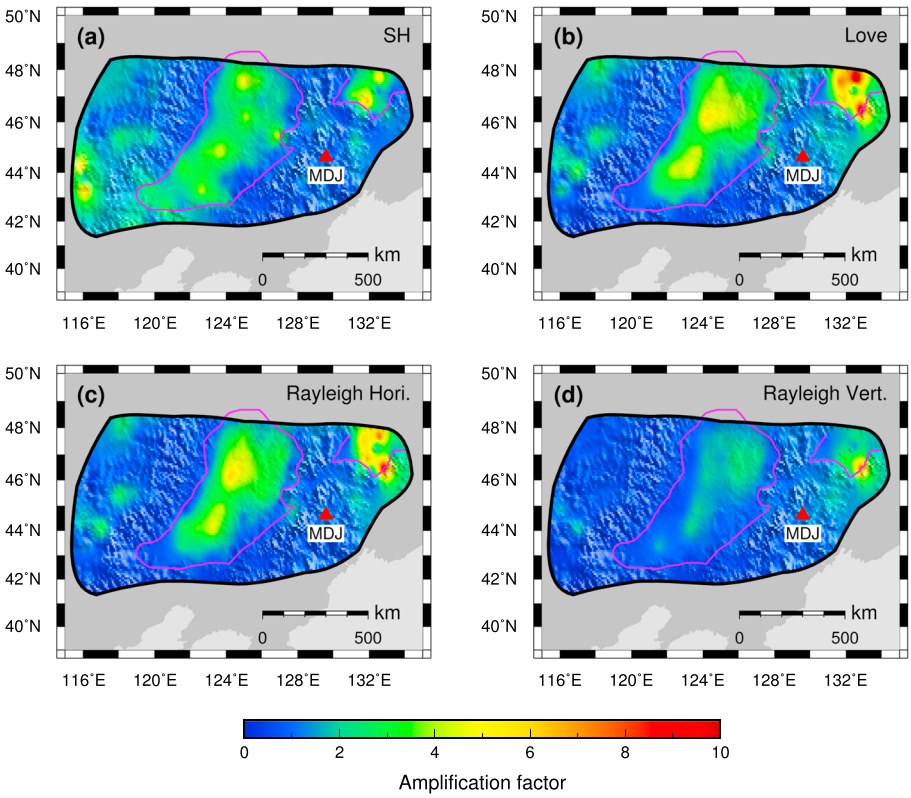

Figure 3. Spatial variability of observed amplification at periods of 2–3 s for (a) vertically incident shear waves, (b) Love waves, (c) horizontal-component Rayleigh waves, and (d) vertical-component Rayleigh waves, respectively. The red triangle denotes the reference station. These maps correlate well with local structure, notably the central Songliao basin and the eastern Sanjiang basin (magenta lines). All of the plots were smoothed using GMT surface (Wessel et al., 2013).

8 and on average by a factor of 4 with respect to the reference site. The northern part of the Songliao basin, which is coincident with the deepest region of the sedimentary basin (Figure S6), appears to be particularly strongly and consistently amplified. Additionally, the amplification of surface waves within the eastern Sanjiang basin at these relatively short periods is surprisingly high, with an amplification factor of more than 8 and locally as high as 15. As expected, comparison of the site amplification between surface waves and shear waves shows prominent differences. While the amplification factors of shear waves are locally as high as 5 at a few sites, surface waves are amplified two to three times more strongly than vertically incident shear waves at most basin sites. Moreover, the site amplifications of shear waves do not exhibit clear correlation with basin depth, implying that the resonance of vertically incident shear waves at these periods is dominated by near-surface soft deposits.

Figure 4 further exhibits the spatial variability of observed amplifications (left panels) in a longer period range (4–5 s), as well as the corresponding modeling results (right panels). Similar to the prominent features in Figure 3, significant site amplification is observed within the two Quaternary sedimentary basins. Nonetheless, the area with strong surface-wave amplification atop the Songliao basin seems to be somewhat smaller for these relatively longer periods (see also Figure S7 for results at a period of 8–9 s), which is again in excellent agreement with where it would be predicted due to its location in the deepest part of the sedimentary basin. While the intensity of amplifications in these maps is slightly different when using a different reference bedrock site, the dominant lateral features still remain. Furthermore, such dominant lateral features of site amplification for both shear waves and surface waves are well explained by the predictions based on the local 1-D structure at each site. Site amplification at some basin sites is moderately overpredicted or underpredicted by a factor up to 2 at relatively short periods (Figures 4 and S8), but the discrepancies between the observations and the predictions are remarkably reduced at longer periods (Figures S9-S12), for which predictions are less affected by details of the velocity model.

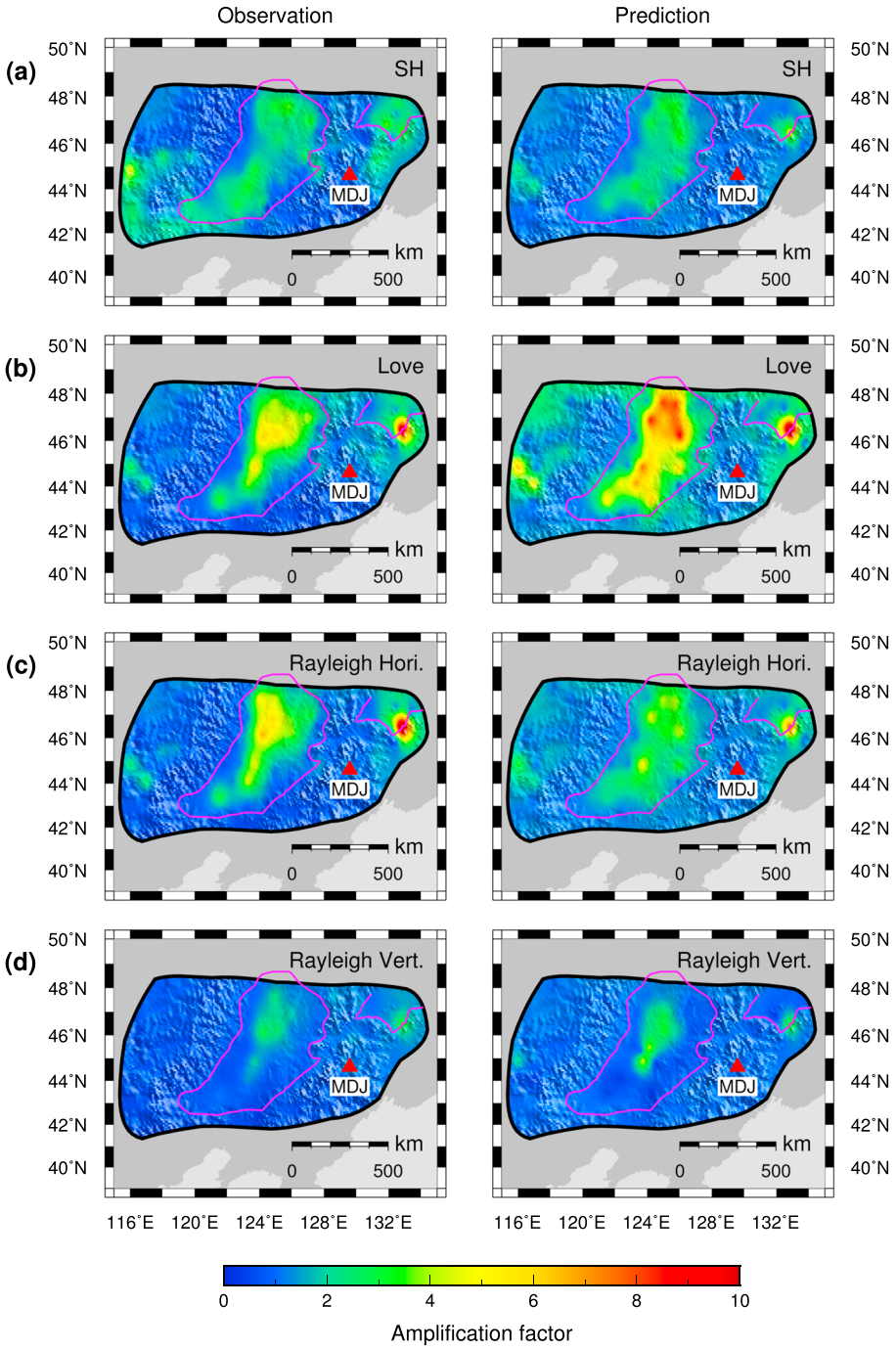

Figure 4. A comparison of spatial variability of observed (left panels) and predicted (right panels) site amplification at periods of 4–5 s, for (a) vertically incident shear waves, (b) Love waves, (c) horizontal-component Rayleigh waves, and (d) vertical-component Rayleigh waves, respectively. The outlines of the Songliao basin and the Sanjiang basin are also shown for reference (magenta lines). All of the plots were smoothed using GMT surface (Wessel et al., 2013).

4. Discussion

As indicated by the spatial variability of site amplification shown in Figures 3 and 4, the areas with substantial amplification are strongly correlated with sedimentary structures. These basins are filled with unconsolidated sediments up to 4 km in thickness (Bao & Niu, 2017; Li et al., 2016). The low-velocity shallow deposits resting on metamorphic basement create a strong contrast in near-surface material properties and thus substantially

increase amplitudes and durations of ground shaking from moderate to large earthquakes. Similar basin resonance effects have been widely documented in other sedimentary basins (e.g., Borcherdt, 1970; Frankel et al., 2009; Galetzka et al., 2015; Kano et al., 2017; Olsen et al., 2006; Pratt et al., 2017). Here we emphasize that surface waves are amplified differently compared to vertically incident shear waves, as indicated by both the observed and predicted site amplifications. Typically, the site amplification of surface waves is stronger by a factor of more than 2. Hence, surface waves, if efficiently excited as in the case of large shallow events, can play a more dominant role in ground shaking, especially at basin sites. Our results are also in general agreement with previous studies. For instance, Bowden and Tsai (2017) reported that the amplification factors in the Los Angeles Basin are 14 and 3.5 for 4-s surface waves and shear waves, respectively, due to the M_w 7.2 El Mayor Cucapah earthquake in 2010. Such different amounts of amplification by local geological structures originate from the distinct nature of wave propagation. As a consequence, if a thorough site characterization at a given site is desired, one must account for the contributions of surface waves, in addition to the standard amplification of vertically propagating shear waves.

It has been reported that 3-D basin effects, for example, scattering and conversion of wave types at sharp basin edges, could significantly aggravate the consequences of ground shaking, especially in the short-period range, leading to concentrated damage in the vicinity of basin edges (Graves et al., 1998; Kawase, 1996; Pilz et al., 2018). Nevertheless, in our results, the good agreement between the observed amplifications and the predictions indicate that the seismic response of long-period ground motions can be largely attributed to local 1-D site effects immediately beneath a given site. The moderate overprediction of Love-wave amplification, as well as the small underprediction of Rayleigh-wave amplification, in the Songliao basin (Figures 4 and S8) is probably due to the large uncertainties in the velocities of the superficial sediments ($<$500 m), which are imperfectly constrained (Li et al., 2016) but are known to have an important influence on the ground motions at the surface, especially in the short-period range ($<$3 s). Similarly, the presence of near-surface soft alluvium might be responsible for the unexpected large site amplification in the Sanjiang basin (Figures 3 and S8). It is noted that the site amplification of both surface waves and shear waves could be further improved by using more accurate 1-D structures.

Our results also validate and demonstrate the usefulness of the semi-analytical theory for surface-wave amplification. This simple method does not address the excitation of surface waves nor realistic 3-D wave propagation effects such as lateral scattering and complex basin reflection (Bowden & Tsai, 2017; Tsai et al., 2017). Still, it can adequately explain the most significant features of surface-wave amplification in the period range of interest, providing valuable insights into key factors that control the spatial variability of site amplification. Note that this approach can also deal with the amplification of higher-mode surface waves, though it is difficult to determine the excitation and relative dominance of higher-mode energy (e.g., Boué et al., 2016). More importantly, this simple method is based solely on the local 1-D geological structure and can be practically incorporated into the current engineering practice of site-specific seismic hazard assessment. Hence, it may find broad application in predicting ground motions of future scenario earthquakes for seismic hazard analysis, providing the foundation for earthquake building codes, as well as ShakeMap applications.

5. Conclusions

We estimated surface-wave amplification across northeast China in the period range 2–10 s, using 12 shallow regional earthquakes off the coast of Japan. Additionally, we also estimated site amplification of vertically incident shear waves with a deep local event beneath the study area. The spatial variations of site amplification for both wave types are strongly correlated with known geological structures. The ground motions of both Love waves and horizontal-component Rayleigh waves within the Songliao basin can be amplified by a maximum factor of 8 and on average by a factor of 4 with respect to the reference site, whereas the site-amplification factors are less than 1.5 at generic rock sites. Furthermore, the area with the strongest amplification in the northern part of the Songliao basin is coincident with the deepest region of the sedimentary basin. However, the site response of surface waves is distinctly different from that of vertically propagating shear waves. In addition to different resonance frequencies, peak amplification factors of surface waves are generally larger than that of shear waves by a factor of more than 2 at most basin sites. Finally, we demonstrated that the most significant site-amplification features of both wave types can be well

explained by the predictions based on the local 1-D structure at each site, in terms of both peak amplification factor and resonance frequency. Our results imply that one needs to account for the contribution of surface waves in future site characterization, which can be practically achieved by incorporating the semi-analytical method for surface-wave amplification into the current engineering practice of seismic hazard assessment.

Acknowledgments

We thank all the people involved in the NECESSArray project for providing the waveform data and Guoliang Li for providing the velocity model used in this study. We also thank Morgan Moschetti and one anonymous reviewer for their constructive comments that improved the quality of this manuscript. Waveform data of the permanent stations were provided by Data Management Centre of the China National Seismic Network at the Institute of Geophysics (SEISDMC, https://doi.org/10.11998/SeisDmc/SN). The NECESSArray data are available from the IRIS data center. This work was jointly supported by the National Key Research and Development Program of China (no. 2017YFC1500300), the National Basic Research Program of China (no. 2015CB250903), the National Natural Science Foundation of China (nos. 41604043 and 41630209), and NSF grants EAR-1453263, SCEC-17061, and EAR-1547228. All the plots were made using the Generic Mapping Tools version 5.4.2 (Wessel et al., 2013).

References

Aki, K., & Richards, P. R. (2002). *Quantitative seismology*. South Orange, NJ: University Science Books.

Asano, K., Sekiguchi, H., Iwata, T., Yoshimi, M., Hayashida, T., Saomoto, H., & Horikawa, H. (2016). Modeling of wave propagation and attenuation in the Osaka sedimentary basin, western Japan, during the 2013 Awaji Island earthquake. *Geophysical Journal International*, *204*, 1678–1694. https://doi.org/10.1093/gji/ggv543

Bao, Y., & Niu, F. (2017). Constraining sedimentary structure using frequency-dependent *P* wave particle motions: A case study of the Songliao basin in NE China. *Journal of Geophysical Research: Solid Earth*, *122*, 9083–9094. https://doi.org/10.1002/2017JB014721

Borcherdt, R. D. (1970). Effects of local geology on ground motion near San Francisco Bay. *Bulletin of the Seismological Society of America*, *60*(1), 29–61.

Borcherdt, R. D., & Gibbs, J. F. (1976). Effects of local geological conditions in the San Francisco Bay region on ground motions and the intensities of the 1906 earthquake. *Bulletin of the Seismological Society of America*, *66*(2), 467–500.

Böse, M., Graves, R. W., Gill, D., Callaghan, S., & Maechling, P. J. (2014). CyberShake-derived ground-motion prediction models for the Los Angeles region with application to earthquake early warning. *Geophysical Journal International*, *198*(3), 1438–1457. https://doi.org/10.1093/gji/ggu198

Boué, P., Denolle, M., Hirata, N., Nakagawa, S., & Beroza, G. C. (2016). Beyond basin resonance: Characterizing wave propagation using a dense array and the ambient seismic field. *Geophysical Journal International*, *206*(2), 1261–1272. https://doi.org/10.1093/gji/ggw205

Bowden, D. C., & Tsai, V. C. (2017). Earthquake ground motion amplification for surface waves. *Geophysical Research Letters*, *44*, 121–127. https://doi.org/10.1002/2016GL071885

Bowden, D. C., Tsai, V. C., & Lin, F. C. (2015). Site amplification, attenuation, and scattering from noise correlation amplitudes across a dense array in Long Beach, CA. *Geophysical Research Letters*, *42*, 1360–1367. https://doi.org/10.1002/2014GL062662

Chaljub, E., Maufroy, E., Moczo, P., Kristek, J., Hollender, F., Bard, P. Y., et al. (2015). 3-D numerical simulations of earthquake ground motion in sedimentary basins: Testing accuracy through stringent models. *Geophysical Journal International*, *201*, 90–111. https://doi.org/10.1093/gji/ggu472

Denolle, M. A., Dunham, E. M., Prieto, G. A., & Beroza, G. C. (2014). Strong ground motion prediction using virtual earthquakes. *Science*, *343*(6169), 399–403. https://doi.org/10.1126/science. 1245678

Denolle, M. A., Miyake, H., Nakagawa, s., Hirata, N., & Beroza, G. C. (2014). Long-period seismic amplification in the Kanto Basin from the ambient seismic field. *Geophysical Research Letters*, *41*, 2319–2325. https://doi.org/10.1002/2014GL059425

Duan, B., Liu, D., & Yin, A. (2017). Seismic shaking in the North China Basin expected from ruptures of a possible seismic gap. *Geophysical Research Letters*, *44*, 4855–4862. https://doi.org/10.1002/2017GL072638

Feng, Z., Jia, C., Xie, X., Zhang, S., Feng, Z., & Cross, T. A. (2010). Tectonostratigraphic units and stratigraphic sequences of the nonmarine Songliao basin, northeast China. *Basin Research*, *22*(1), 79–95. https://doi.org/10.1111/j.1365-2117.2009.00445.x

Frankel, A., Stephenson, W., & Carver, D. (2009). Sedimentary basin effects in Seattle, Washington: Ground-motion observations and 3D simulations. *Bulletin of the Seismological Society of America*, *99*(3), 1579–1611. https://doi.org/10.1785/0120080203

Galetzka, J., Melgar, D., Genrich, J. F., Geng, J., Owen, S., Lindsey, E. O., et al. (2015). Slip pulse and resonance of the Kathmandu basin during the 2015 Gorkha earthquake, Nepal. *Science*, *349*(6252), 1091–1095. https://doi.org/10.1126/science. aac6383

Graves, R. W., Pitarka, A., & Somerville, P. G. (1998). Ground-motion amplification in the Santa Monica area: Effects of shallow basin-edge structure. *Bulletin of the Seismological Society of America*, *88*(5), 1224–1242.

Haskell, N. A. (1953). The dispersion of surface waves on multilayered media. *Bulletin of the Seismological Society of America*, *43*(1), 17–34.

Hatayama, K. (2008). Lessons from the 2003 Tokachi-oki, Japan, earthquake for prediction of long-period strong ground motions and sloshing damage to oil storage tanks. *Journal of Seismology*, *12*(2), 255–263. https://doi.org/10.1007/s10950-007-9066-y

Imperatory, W., & Mai, P. M. (2015). The role of topography and lateral velocity heterogeneities on near-source scattering and ground-motion variability. *Geophysical Journal International*, *202*(3), 2163–2181. https://doi.org/10.1093/gji/ggv281

Iwaki, A., & Iwaka, T. (2010). Simulation of long-period ground motion in the Osaka sedimentary basin: Performance estimation and the basin structure effects. *Geophysical Journal International*, *181*, 1062–1076. https://doi.org/10.1111/j.1365-246X.2010.04556.x

Kano, M., Nagao, H., Nagata, K., Ito, S., Sakai, S., Nakagawa, S., et al. (2017). Seismic wavefield imaging of long-period ground motion in the Tokyo metropolitan area, Japan. *Journal of Geophysical Research: Solid Earth*, *122*, 5435–5451. https://doi.org/10.1002/2017JB014276

Kawase, H. (1996). The cause of the damage belt in Kobe: "The basin-edge effect", constructive interference of the direct *S*-wave with the basin-induced diffracted/Rayleigh waves. *Seismological Research Letters*, *67*(5), 25–34. https://doi.org/10.1785/gssrl.67.5.25

Koketsu, K., & Kikuchi, M. (2000). Propagation of seismic ground motion in the Kanto basin, Japan. *Science*, *288*(5469), 1237–1239. https://doi.org/10.1126/science.288.5469.1237

Kramer, S. L. (1996). *Geotechnical earthquake engineering*. Upper Saddle River, NJ: Prentice Hall.

Li, G., Chen, H., Niu, F., Guo, Z., Yang, Y., & Xie, J. (2016). Measurement of Rayleigh wave ellipticity and its application to the joint inversion of high-resolution *S* wave velocity structure beneath northeast China. *Journal of Geophysical Research: Solid Earth*, *121*, 864–880. https://doi.org/10.1002/2015JB012459

Moschetti, M. P., Hartzell, S., Ramírez-Guzmán, L., Frankel, A. D., Angster, S. J., & Stephenson, W. J. (2017). 3D ground-motion simulations of M_w 7 earthquakes on the Salt Lake City segment of the Wasatch fault zone: Variability of long-period ($T \geq 1$ s) ground motions and sensitivity to kinematic rupture parameters. *Bulletin of the Seismological Society of America*, *107*(4), 1704–1723. https://doi.org/10.1785/0120160307

Nigam, N. C., & Jennings, P. C. (1969). Calculation of response spectra from strong-motion earthquake records. *Bulletin of the Seismological Society of America*, *59*(2), 909–922.

Olsen, K. B. (2000). Site amplification in the Los Angeles basin from three-dimensional modeling of ground motion. *Bulletin of the Seismological Society of America*, *90*(6B), S77–S94. https://doi.org/10.1785/0120000506

Olsen, K. B., Day, S. M., Minster, J. B., Cui, Y., Chourasia, A., Faerman, M., et al. (2006). Strong shaking in Los Angeles expected from southern San Andreas earthquake. *Geophysical Research Letters*, *33*, L07305. https://doi.org/10.1029/2005GL025472

Pilz, M., Parolai, S., Petrovic, B., Silacheva, N., Abakanov, T., Orunbaev, S., & Moldobekov, B. (2018). Basin-edge generated Rayleigh waves in the Almaty basin and corresponding consequences for ground motion amplification. *Geophysical Journal International*, *213*(1), 301–316. https://doi.org/10.1093/gji/ggx555

Pilz, M., Parolai, S., Stupazzini, M., Paolucci, r., & Zschau, J. (2011). Modeling basin effects on earthquake ground motion in the Santiago de Chile basin by a spectral element code. *Geophysical Journal International*, *187*(2), 929–945. https://doi.org/10.1111/j.1365-246X.2011.05183.x

Pratt, T. L., Horton, J. W. Jr., Muñoz, J., Hough, S. E., Chapman, M. C., & Olgun, C. G. (2017). Amplification of earthquake ground motions in Washington, DC, and implications for hazard assessments in central and eastern North America. *Geophysical Research Letters*, *44*, 12,150–12,160. https://doi.org/10.1002/2017GL075517

Roten, D., Fäh, D., & Bonilla, L. F. (2013). High-frequency ground motion amplification during the 2011 Tohoku earthquake explained by soil dilatancy. *Geophysical Journal International*, *193*(2), 898–904. https://doi.org/10.1093/gji/ggt001

Steidl, J. H. (2000). Site response in southern California for probabilistic seismic hazard analysis. *Bulletin of the Seismological Society of America*, *90*(6B), S149–S169. https://doi.org/10.1785/0120000504

Takemura, S., Akatsu, M., Masuda, K., Kajikawa, K., & Yoshimoto, K. (2015). Long-period ground motions in a laterally inhomogeneous large sedimentary basin: Observations and model simulations of long-period surface waves in the northern Kanto Basin, Japan. *Earth, Planets and Space*, *67*(1), 33. https://doi.org/10.1186/s40623-015-0201-7

Tao, K., Niu, F., Ning, J., Chen, Y. J., Grand, S., Kawakatsu, H., et al. (2014). Crustal structure beneath NE China imaged by NECESSArray receiver function data. *Earth and Planetary Science Letters*, *398*, 48–57. https://doi.org/10.1016/j.epsl. 2014.04.043

Tromp, J., & Dahlen, F. A. (1992). Variational principles for surface wave propagation on a laterally heterogeneous earth – II. Frequency-domain JWKB theory. *Geophysical Journal International*, *109*(3), 599–619. https://doi.org/10.1111/j.1365-246X.1992.tb00120.x

Tsai, V. C., Bowden, D. C., & Kanamori, H. (2017). Explaining extreme ground motion in Osaka basin during the 2011 Tohoku earthquake. *Geophysical Research Letters*, *44*, 7239–7244. https://doi.org/10.1002/2017GL074120

Viens, L., Koketsu, K., Miyake, H., Sakai, S., & Nakagawa, S. (2016). Basin-scale Green's functions from the ambient seismic field recorded by MeSO-net stations. *Journal of Geophysical Research: Solid Earth*, *121*, 2507–2520. https://doi.org/10.1002/2016JB012796

Wessel, P., Smith, W. H. F., Scharroo, R., Luis, J. F., & Wobbe, F. (2013). Generic mapping tools: Improved version released. *Eos, Transactions American Geophysical Union*, *94*(45), 409–410. https://doi.org/10.1002/2013EO450001